Nanocomposite PAAm/Methyl Cellulose/Montmorillonite Hydrogel: Evidence of Synergistic Effects for the Slow Release of Fertilizers

ARTICLE *in* JOURNAL OF AGRICULTURAL AND FOOD CHEMISTRY · JULY 2013

Impact Factor: 2.91 · DOI: 10.1021/jf401273n · Source: PubMed

4 AUTHORS, INCLUDING:

Fauze Aouada
São Paulo State University
44 PUBLICATIONS **569** CITATIONS
SEE PROFILE

Caue Ribeiro
Brazilian Agricultural Research Corporation (…
123 PUBLICATIONS **1,739** CITATIONS
SEE PROFILE

Journal of Applied Polymer Science

Study of a Nanocomposite Starch-Clay for Slow-Release of Herbicides: Evidence of Synergistic Effects Between the Biodegradable Matrix and Exfoliated Clay on Herbicide Release Control

Amanda S. Giroto,[1] Adriana de Campos,[2] Elaine I. Pereira,[1] Camila C. T. Cruz,[1] José M. Marconcini,[2] Caue Ribeiro[2]

[1]Universidade Federal de São Carlos, Departamento de Química - Rod. Washington Luiz, km 235 – CEP: 13565-905, São Carlos SP, Brazil

[2]EMBRAPA Instrumentação, Rua XV de Novembro, 1452 – CEP: 13560-970 CP: 741, São Carlos SP, Brazil

Correspondence to: C. Ribeiro (E-mail: caue.ribeiro@embrapa.br)

ABSTRACT: In this article a nanocomposite based on starch gel, a renewable polymer, and montmorillonite clay (MMT) is proposed as a host system for the slow-delivery of a hydrophobic herbicide loaded in very high contents (50% in total weight), where the nanocomposite structure controls the release by imposing diffusional barriers to the active compound. The herbicide release rate in water showed that nanocomposites presented higher retentions than the neat samples (herbicide-loaded starch or MMT), revealing a cooperative or synergic effect between the constituents. Biodegradation essays also revealed this cooperative behavior, showing longer biodegradation periods for the nanocomposite than the pristine materials. Also, a two-step release was noticed, where the first step was controlled by starch (short periods) and the second was played by MMT (longer times). The nanocomposite structural analysis gave evidence that the release behavior is governed by the interaction between the constituents, even at very high herbicide contents.
 J. Appl. Polym. Sci. **2014**, *131*, 41188.

KEYWORDS: biopolymers and renewable polymers; clay; composites; drug delivery systems

Received 28 March 2014; accepted 18 June 2014
DOI: 10.1002/app.41188

INTRODUCTION

The high values currently achieved in agricultural production are also linked to pesticide use, coupled with factors like favorable weather and fertilizer application. Generally, a pesticide is any agent used to kill or control insects, weeds, rodents, fungi, bacteria, or other organisms.[1] According to Arias-Estevez et al.[2] 60%–70% of the pesticides used in agricultural fields do not reach the target surface and this fraction is lost in the environment. Therefore, pesticides have become one of the most important organic pollutants in water and soil, causing concerns with respect to their effects on the environment and human life.[3] However, the controlled release of agrochemicals is a key strategy to reduce the applied amount of these products, reducing their impact on the environment and human health, besides reducing the agricultural costs.[4–6]

Pesticide encapsulation into biopolymer starch has received increasing attention.[7–9] At present, the release is mainly governed by diffusional processes: when starch granules are applied to the soil, they imbibe water, swell, and the encapsulated compound diffuses out of the starch matrix.[7] Also, its biodegradability will interfere in the final release, since during this process, the capsule structure will fall and, consequently, the compound will be released. However, in this strategy it is difficult to control the releasing process, since it is solely governed by the matrix properties and by their interactions with the active compound. Since starch is a hydrophilic material, poor water-soluble pesticides may be inadequate for this strategy. This is the case with ametryne, which is a herbicide (pesticide for the control of weeds) belonging to the triazine group, along with atrazine and simazine, widely used in sugar cane, rice, corn, and soybean productions.[10]

Thus, an attractive way to suit this matrix to a wide range of compounds of interest and modify its diffusional process is to prepare a nanocomposite where exfoliated clay is used to impose diffusional barriers to the molecular movement.[11] Additionally, it is well known that starch-based nanocomposites have better mechanical properties than neat starch.[12] The use of exfoliated clays as filler materials has received increasing attention and large numbers of works have been pursued in examining the preparation and characterization of these nanocomposites, especially in the modification of diffusional properties. Aspects such as the internal pore structure and the sorption of the compound to the clay mineral have been taken into account in

Table I. Chemical Composition of Montmorillonite Clay

Component	% component
SiO_2	57.50
Al_2O_3	18.30
Fe_2O_3	8.23
CaO	0.71
MgO	2.62
Na_2O	2.49
trace	1.89
Loss of ignition	7.18

previous studies[13,14] although to the best of our knowledge, few studies using starch and ametryne and clay composites have been produced.

In the present investigation, nanocomposite based on clay exfoliated into a starch matrix and incorporating a significant amount of ametryne, for the release control of this herbicide has been studied. The results showed an interesting synergistic effect, where the starch matrix acts controlling the short time release and the clay modifies this behavior into longer times.

EXPERIMENTAL

Materials

The raw materials used as basis for the nanocomposite formulations were ametryne (Metrimex 500 SC, NUFARM), montmorillonite clay (MMT) without purification (Bentonita, Drescon S/A, Drilling Products), and corn starch (Amidex 3001–70% amylopectin and 30% amylose), kindly supplied by Corn Products Brazil. The clay material (average particle size of 230 nm) was used as received, and the chemical composition obtained by X-ray fluorescence spectroscopy (SGS Geosol Laboratorios Ltda, Brazil) is listed in Table I.

Preparation of Nanocomposites

The nanocomposites were obtained by starch gelatinization (5 wt %), through dispersion in distilled water in a beaker and mechanical stirring for 15 min. The gelatinization process was done by keeping the dispersed starch at about 90°C for 30 min under stirring, until a sticky starch paste was formed. Then, the temperature was decreased to 70°C and the MMT and/or ametryne were incorporated with the gelatinized starch gel. Surfactants or dispersants were not necessary for the complete exfoliation, since MMT clay is hydrophilic. The mixed gel was kept at 30°C with air circulation for at least 72 h to obtain a solid gel. Subsequently, the materials were obtained as a powder by milling in ball mill during 24 h (SERVITECH, CT 242). All the nanocomposites groups were prepared using the same procedure, at different ratios (w/w basis) of starch gel and MMT as shown in Table II. For the herbicide encapsulation, the desired herbicide amount was added at the same moment as the MMT, adding 50% in mass of ametryne (related to the total mass of the nanocomposite). Table II describes the details of the formulations prepared. The final water content in the nanocomposites was 4% (Table III). All the nanocomposites groups were prepared using the same procedure, at different ratios (w/w basis) of starch gel and MMT as shown in Table II.

Characterization

X-ray Diffraction. X-ray patterns (XRD) were obtained using a Shimadzu XRD 6000 diffractometer. The relative intensity was recorded in a diffraction range (2θ) of 3°–40°, using a Cu $K\alpha$ incident beam ($\lambda = 0.1546$ nm). The scanning speed was 1 min^{-1}, and the voltage and current of the X-ray tubes were 30 kV and 30 mA, respectively. The corresponding "d" interplanar basal spacing of the MMT was computed from Bragg's diffraction equation, $2d \cdot \sin\theta = n \cdot \lambda$, "$n$" (=1) being the order of reflection and "θ" the angle of refraction.

SEM Measurements. The morphology and relative elemental concentration of the samples were analyzed by scanning electron microscopy (SEM) (JEOL microscope, model JSM 6510) equipped with an energy dispersive analysis system of X-ray spectrometer-EDX (Thermo Scientific NSS coupled or linked). The sample was dispersed over carbon tape pasted on the surface of a metallic disk (stub). The disk was then coated with gold in an ionization chamber (BALTEC Med. 020) and analyzed.

Thermogravimetric Analysis. Thermal degradation was evaluated using a TGA Q500 thermogravimetric analyzer (TA Instruments, New Castle, DE) under the following conditions: weight 10.00 ± 0.50 mg; synthetic air flow 60 mL/min; heating rate 100°C/min; and temperature range of 25°C–600°C.

Fourier Transform Infrared (FTIR) Measurements. The spectroscopic analyses in the infrared region of the polymers and composites were performed on a KBr disk (5/200 mg) in the range of 4000–500 cm^{-1}. The FTIR spectra data was obtained using Shimadzu FTIR-8300 instrument.

Water Absorption of the Composites. Water absorption tests were conducted in accordance with ASTM D570-98.[15] The specimens were dried at 75°C for 4 h, and placed in test tubes of 25 mL until 2.5 mL of the mark, and the volume was completed with distilled water. The experiment was conducted at 20°C and filled volume by the samples were recorded at

Table II. Mix Design Used in the Production of Composites

Samples	Amount (g)						
Starch	15	15	15	15	15	15	15
MMT	0	15	30	60	15	30	60
Amet	15	0	0	0	30	45	75
Designate	St/Amet 1 : 1	St/MMT 1 : 1	St/MMT 1 : 2	St/MMT 1 : 4	1 : 1 : 2 Amet	1 : 2 : 3 Amet	1 : 4 : 5 Amet

Table III. Stages of Thermoxidative Degradation of Ametryne and Nanocomposites

Samples	Total loss (%)	Water content (%)	T_{onset} (°C) 1st stage	T_{onset} (°C) 2st stage	T_{onset} (°C) 3st stage
Ametryne	99	-	178	-	-
MMT	12	7	-	-	409
MMT/Amet	16	7	175	-	-
Starch gel	100	4	-	287	-
St/Amet 1 : 1	100	4	174	281	436
St/MMT 1 : 1	43	7	-	255	-
St/MMT 1 : 2	28	7	-	242	-
St/MMT 1 : 4	32	7	-	225	-
1 : 1 : 2 Amet	55	4	117	228	-
1 : 2 : 3 Amet	52	4	141	246	-
1 : 4 : 5 Amet	53	4	156	266	-

different time intervals up to complete 76 h. The water absorption were determined using the eq. (1):

$$\text{Water absorption } (\%) = [(V_t - V_o)/V_o] \times 100 \quad (1)$$

where V_o is the initial volume (prior to exposure to moisture) and V_t is the samples volume measured after certain intervals of time "t" to reach the equilibrium state.

Kinetic Swelling Parameters. For the calculation of kinetic swelling parameters, time measurements ($F \times t$) in solutions pH = 7.0 were done, adapted from the method proposed by Aouada et al.[16] For each $F \times t$ curve, the diffusional exponent (n) and diffusion constant (k) were calculated using eq. (2):

$$F = M_t/M_{eq} = k \cdot t^n \quad (2)$$

where M_{eq} is the mass of nanocomposites at equilibrium swelling and t is the time. k is known as a diffusion constant and depends on the material and swelling place. According to Rigter and Peppas[17] the eq. (2) can be applied from the early stages to 60% of $F \times t$ curve. The increased swelling degree with time is almost linear, and after the 60% stage, the swelling no longer follows this trend. Generally, the swelling degrees will not suffer more variation over time (reaching the equilibrium state). In order to obtain the value of n and k, an ln $F \times$ ln t graph was plotted, where the value of diffusional exponent n is the slope of the curve and ln k is the intercept.

Release Rate of Active Components in Water. A test in aqueous medium was performed, adapted from Tomaszewska and Jarosiewicz[18] and Pereira et al.[11] where the release rate of ametryne as a function of time at room temperature was compared for each composite. An apparatus of drug delivery system was designed, in which a known mass of the material was placed in a beaker immersed in aqueous medium, with external stirring of the beaker contents, to ensure that the content of ametryne measured in the liquid medium corresponded to the diffusion into the medium and not due to the mechanical action of the stirrer. The beakers were sealed with plastic wrap to reduce evaporation losses. Aliquots were collected at different time intervals, over 6 days. For comparison, a test with pure ametryne was also performed as a control experiment. The determination of the ametryne concentration in solution was done by UV−vis spectrophotometry (Shimadzu-1601PC) based on a calibration curve previously build in a specific wavelength ($\lambda = 223$ nm). After the measurements at each time, the aliquots were returned to the original solution, in order to avoid system volume changes. Thus, a curve of ametryne concentration in solution versus release time was obtained. Each experiment was repeated for the three samples of each system, in simultaneous measurements made under the same conditions for all the samples.

Biodegradation Tests. About 2.0 g of each sample in a fine consistency of powder was mixed with 50 g of compost soil under appropriate conditions in a 500 mL reaction chamber (respirometer) at 28°C for almost 60 days. The accumulation of CO_2 was monitored, following Brazilian technical standard.[19] Each sample was run in triplicates and averaged. Samples were accompanied by at least triplicate blanks (compost alone) to measure the background CO_2. The carbon dioxide produced during the microbial activity was captured by a 0.20M KOH solution (10 mL) located by the side of the biometer flasks. Periodically, the KOH solution was removed and 1 mL of 0.5M barium chloride solution was added. The residual KOH was titrated with 0.1M HCl standardized solution. Details of the Brazilian standard[19] are described in previous articles.[20–22]

RESULTS AND DISCUSSION

XRD was useful to evaluate the exfoliation and intercalation of ametryne into montmorillonite and starch, as well as the interlamellar distance of their crystals, monitored by the displacement of the diffraction angle d_{001}, characteristic of basal separation of MMT, as shown in Figure 1.

According to Bragg's law, the diffraction angle θ and the interplanar distance d are inversely proportional, that is, a decrease in diffraction angle means an increase in the interplanar distance. As shown in Figure 1(a), a decrease was observed in the intensity of d_{001} for all the nanocomposites, meaning that a significant part of the montmorillonite underwent exfoliation after

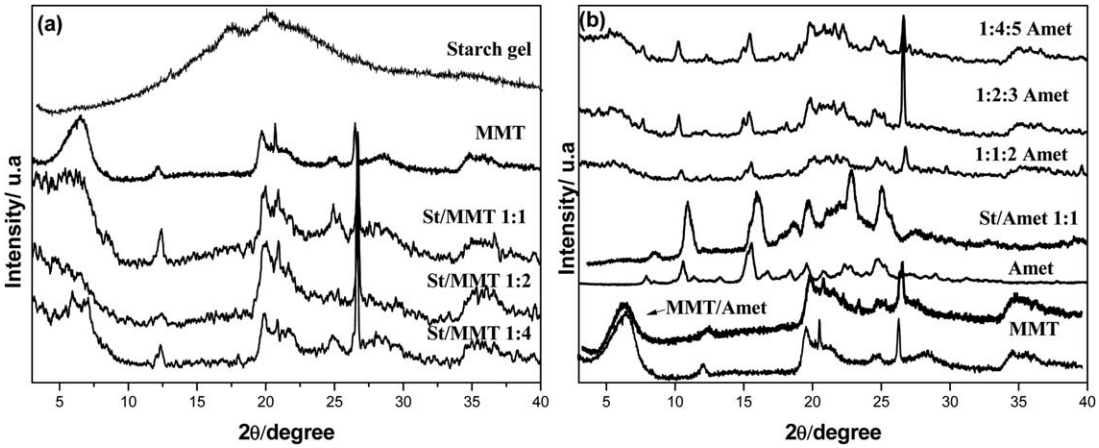

Figure 1. X-ray diffraction (XRD) patterns (**a**) of the starch gel and MMT and of the nanocomposites St/MMT 1 : 1, St/MMT 1 : 2, St/MMT 1 : 4 and (**b**) ametryne (Amet) and nanocomposites 1 : 1 : 2 Amet; 1 : 2 : 3 Amet; 1 : 4 : 5 Amet; and St/Amet 1 : 1.

mixing with the starch. However, it is important to notice that the exfoliation may be attributed to the starch presence, since in the sample produced only with ametryne and MMT (MMT/Amet) a reduction or displacement was not observed in the diffraction peaks, that is, the herbicide did not influence the clay exfoliation. The exfoliation of layered clay mineral is promoted by water. However, after drying the material, the lamellar structure is restored. In the composite preparation, to keep the exfoliated structure, the formation of a polymeric network in the exfoliated state would assure this state. In this study, the formation of amylose network, present in the starch, is holding delamination of MMT particles lamellae. Also, almost the same behavior was observed for the nanocomposites containing ametryne. Figure 1(b) shows that the ametryne is crystalline even in the nanocomposites, identified by the peaks at 10.3° and 15.3°.

SEM was applied to analyze the morphological aspects of pure starch gel, MMT, and nanocomposites (Figure 2). In Figure 2(a) it is observed that the starch gel exhibited a relatively homogeneous surface, showing an almost amorphous structure, in accordance with the XRD patterns. Compared with the pure MMT morphology [Figure 2(b)], was observed morphology changes after the formation of the composites (SEM images d, e, and f). Besün et al.[23] studied the structure of starch and MMT gels, observing that there is a high affinity of starch and MMT surface. This affinity is due to hydration water of the MMT and groups hydroxyl of the starch. However, it is possible to verify the presence of clay platelets when MMT is in higher amount [Figure 2(f)]. When the clay and the herbicide are incorporated into the starch gel [Figure 2(g–i)], defects at interface are observed with the presence of some crystals. These are probably related to ametryne crystals encapsulated by starch and the MMT matrix. A good herbicide dispersion is observed across the nanocomposite surface, furthermore verified the presence of ametryne crystals. In the figures regarding samples without ametryne, these pores are not observed. This is an indicative that the herbicide may be encapsulated into the structure, occupying those void spaces. In order to confirm the ametryne presence, energy dispersive analysis was performed, verifying the sulfur peak intensity, present in the ametryne sample [Figure 2(l)].

Figure 3 and Table III show the thermo-oxidative degradation of the nanocomposites. The final residue in all the cases refers to the MMT phase, when present. As references for the thermal transitions, the herbicide characterization evidences that its mass loss starts at 169°C. The starch gel presents main mass loss starting at 280°C, where the mass loss in the range 25°C–220°C are attributed to the evaporation of volatiles, as water.[26,27] A decrease (about 43°C) was observed in the thermal stability of starch present in St/MMT composites, especially for the samples with contents higher than 1 : 1. This may be due to minor interactions between polymer chains intercalated by MMT. These interactions were confirmed by FTIR (Figure 4). However, it is observed that the decrease (about 54°C to 1 : 1 : 2 Amet) of thermal stability is more pronounced when ametryne is present in the composite. In this case, it is suggested that there are interactions between starch and ametryne and MMT with ametryne, influencing the shift to lower temperatures. Studies[14,22,23] shows that MMT addition improves the thermal stability of composites with polymeric matrix. However, Ibrahim,[24] found that there are limits to the clay content that can be added to improve these thermal properties, giving that the amount of MMT used for the preparation of composite starch–MMT is above this threshold. Another reason for the decrease in thermal stability is in thermal degradation of the starch, which can produce small polar molecules (CO, H_2O, CH_2O) accelerating ametryne chainsbreakdown.[25]

Infrared spectroscopy was used to characterize the structural changes and interactions in the samples studied, as shown in Figure 4. The starch gel band at 3400 cm^{-1} is attributed to O—H group stretching and the band at 2935 cm^{-1} to the stretching of the C—H groups. In the Figure 4(a), it is shown that the MMT main bands are related to Si—O vibrations in 900 cm^{-1} and O—H stretching in 1650 cm^{-1}. In this clay there are two hydroxyls kinds: there active hydroxyl in 3650 cm^{-1} located in the outer layers of the clay and the non-reactive in 3440 cm^{-1} located with compensation cations. It was verified in the St/MMT spectrums that the hydroxyl groups of starch are interacting with their active hydroxyls of MMT due to the displacement of the band at 3400 cm^{-1}, attributed to O—H group

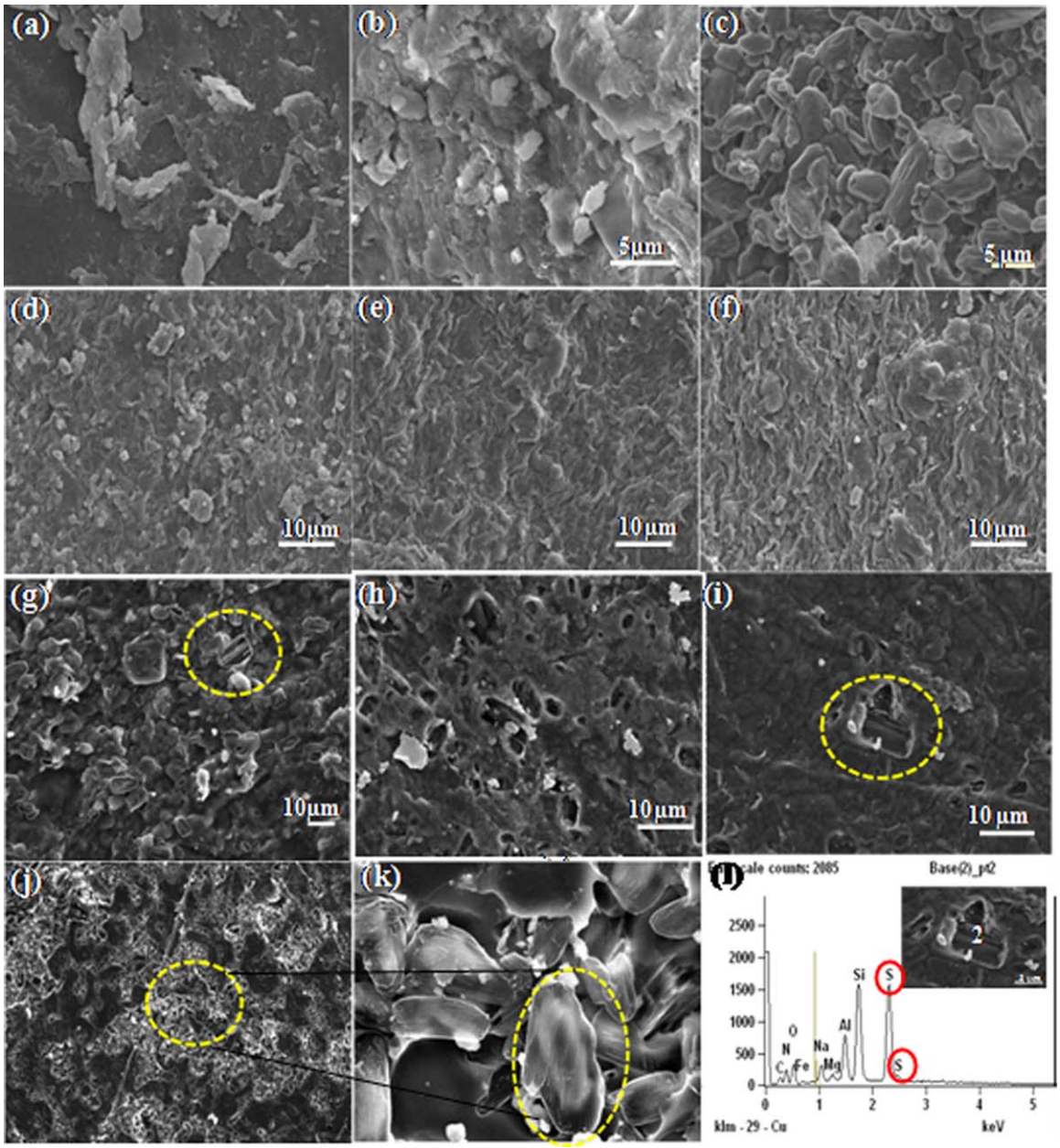

Figure 2. SEM micrographs of (**a**) MMT, (**b**) starch gel, (**c**) ametryne, (**d**) St/MMT 1 : 1, (**e**) St/MMT 1 : 2, (**f**) St/MMT 1 : 4, (**g**) 1 : 1 : 2 Amet, (**h**) 1 : 2 : 3 Amet, (**i**) 1 : 4 : 5 Amet, (**j**) St/Amet 1 : 1, (**k**) enlarged image of St/Amet 1 : 1, and (**l**) of energy dispersive X-ray analysis from the sample 1 : 4 : 5 Amet. [Color figure can be viewed in the online issue, which is available at wileyonlinelibrary.com.]

of starch. It was also observed that the peak at 1640 cm^{-1} of starch, attributed to stretching of O—H, had been suppressed. Three characteristic bands can be observed in the pure ametryne spectrum. The band at 3240 cm^{-1} corresponds to N—H bond stretching present in the amine functional group of the herbicide molecule, while bands at 2969 cm^{-1} and 1520 cm^{-1} are related to the alkyl group C—H bond stretching, and angular deformation of the amine N—H bond, respectively.[28] Ametryne incorporated into the St/MMT nanocomposites shifted the band at 2969–2975 cm^{-1}, which is attributed to C—H groups of ametryne due to the interaction with starch. The band at 1640 cm^{-1} is attributed to rocking vibration of the —OH groups in starch water, as also observed by Mano et al.[29] This band was shifted to 1600 cm^{-1} in the St/MMT/Amet nanocomposites. These displacements indicated possible ionic interactions and hydrogen bonding between both components of the nanocomposites, due to the negative charges of ametryne with positive charges of the MMT in the starch gel, according to that observed in DTG characterization. Bands related to the presence of free clay were verified in Figure 4(b). Furthermore, due to the high concentration of clay in the nanocomposite it is observed a decrease in the band related interactions among the hydroxyl groups of the composite and reappearance of vibration N—H band. This result indicates that the ametryne is less linked

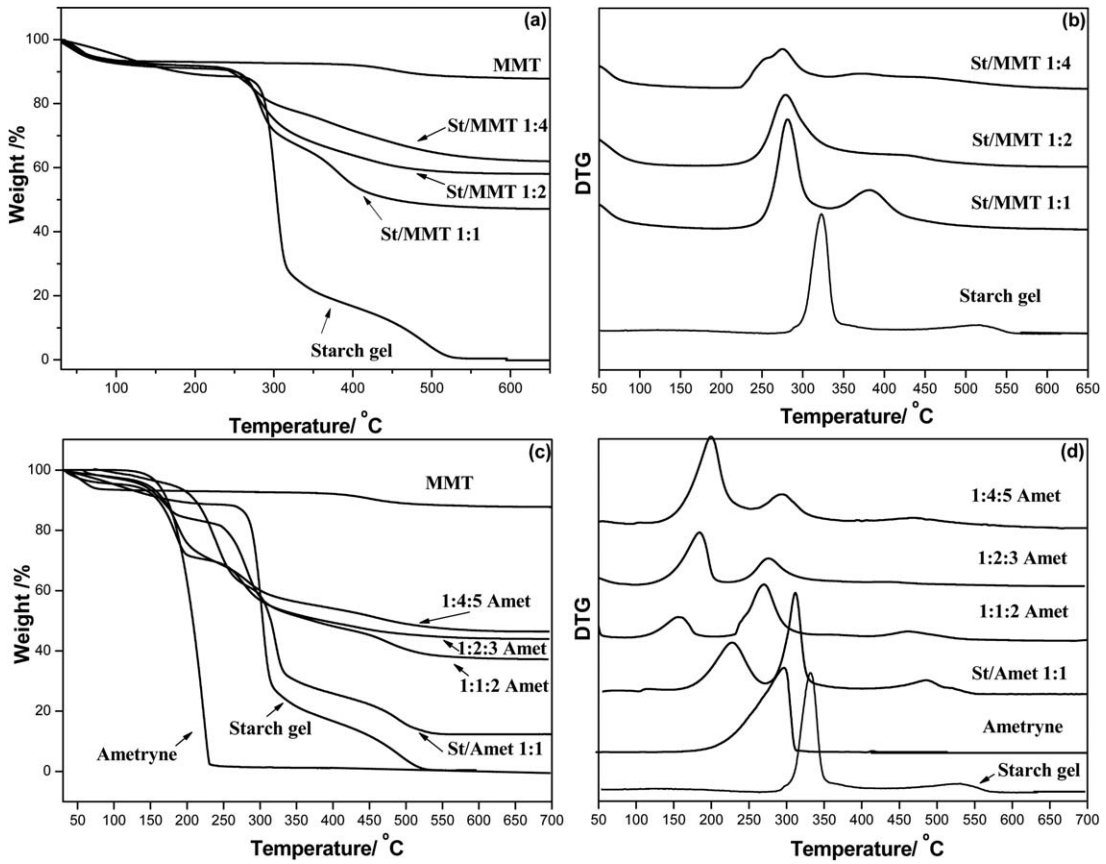

Figure 3. TGA and DTA results: (**a**) TGA of starch gel, montmorillonite, and the nanocomposites containing only starch and montmorillonite in different contents, monitored at 10°C/min under a synthetic air flow atmosphere (**b**) DTA of samples in (a), (**c**) TGA results of ametryne and nanocomposites containing herbicide and (**d**) DTA of samples of (c).

to starch and possibly linked by adsorption in clay. Senesi and Testini,[30] studying humic acid and triazine interactions, observed a sharp simultaneous increase and broadening of the superimposed bands in the 1660–1600 cm^{-1} range, due to the anti-symmetric stretching of COO— and also partly to the N—H deformation bending of secondary amino-groups and C═N stretching vibrations of the heterocyclic ring of adsorbed s-triazine. According to Wing et al.[31] gelatinized starch is cross-linked through the natural process of retrogradation after herbicide addition. During the gelatinization time, when a starch granule comes into contact with the surface of montmorillonite lamellae, it attracts the adsorbed water molecules. In addition,

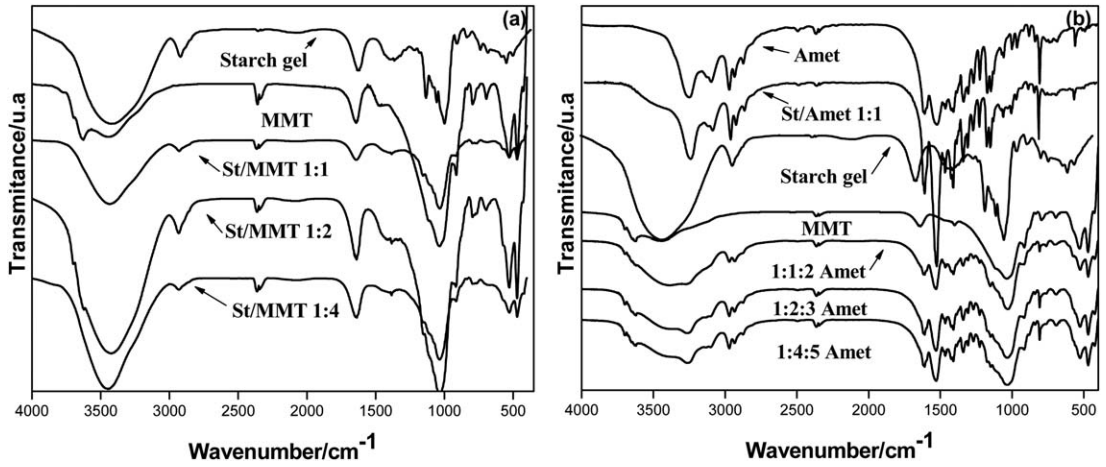

Figure 4. FTIR spectra of (**a**) starch gel, MMT, and the nanocomposites in different contents and (**b**) ametryne and nanocomposites containing herbicide.

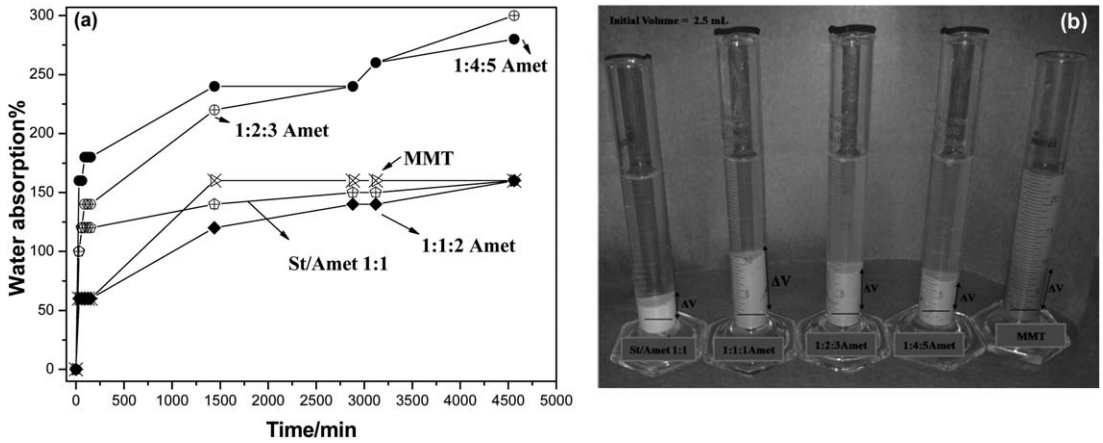

Figure 5. Results of the analysis of water absorption for montmorillonite and nanocomposites containing ametryne (**a**), and (**b**) illustration of the experiment.

it forms hydrogen bonds with the oxygen atoms on the clay mineral surface. Heating during the gel formation favors water desorption from the clay mineral surface and the breaking of the hydrogen bonds in the crystallites within the granules.[23]

The water uptake test investigated the influence of hygroscopic properties of the starch and clay nanocomposites. The amounts of water uptake are shown in Figure 5. All samples have increased in volume over time, as expected. It can be seen that there was two different speed of swelling. It is believed that the first water absorption is related to starch and at longer times, the hydroxyls on the MMT surface become responsible for the swelling behavior as seen in Figure 5. This behavior reflects the influence of the hydroxyl groups present in the components of the composites, starch, and MMT. Starch gel composite has great rate swelling, forming a layer of high viscosity in the polymer–water interface. This viscous layer thickness increases as the swelling progresses, or hydration. As expected, the swelling behavior increases according to the MMT amount in the composites. The samples that have higher amounts of MMT are responsible for the higher values of swelling, such as the composites 1 : 2 : 3 Amet and 1 : 4 : 5 Amet, which presented water uptake around 300% and 294%. Consequently, the diffusion of the herbicide is also determined by the rate of swelling of the nanocomposite.

The release curves (Figure 6) were analyzed in order to obtain information about the possible mechanisms governing the release process, according to Grillo et al.[28] Figure 6(a) shows the first release stage for all the produced samples, compared with the ametryne dissolution in water, 90% completed after 3 h. The sample St/Amet 1 : 1 presented behavior closer to neat ametryne. In just 20 min, the starch granules absorb water enough to start releasing the ametryne. On the other hand, when using the material prepared from adsorption of Amet into the MMT has a high retention of this ametryne, releasing only 40% of the total after 27 h immersed. This indicates that the use of only starch or MMT not control the release of ametryne, once the ideal behavior intermediate is between the two extremes mentioned. However, at higher release times (up to 160 h), it was observed that the amount released by the MMT/Amet material was almost stable, indicating that the retention mechanism is a single step process, probably associated to the ametryne adsorption on the MMT lamellae. In those conditions, it is noteworthy that the (1 : 1 : 2, 1 : 2 : 3, and 1 : 4 : 5 Amet) nanocomposites showed a two-step process, that is, after 22 h; a

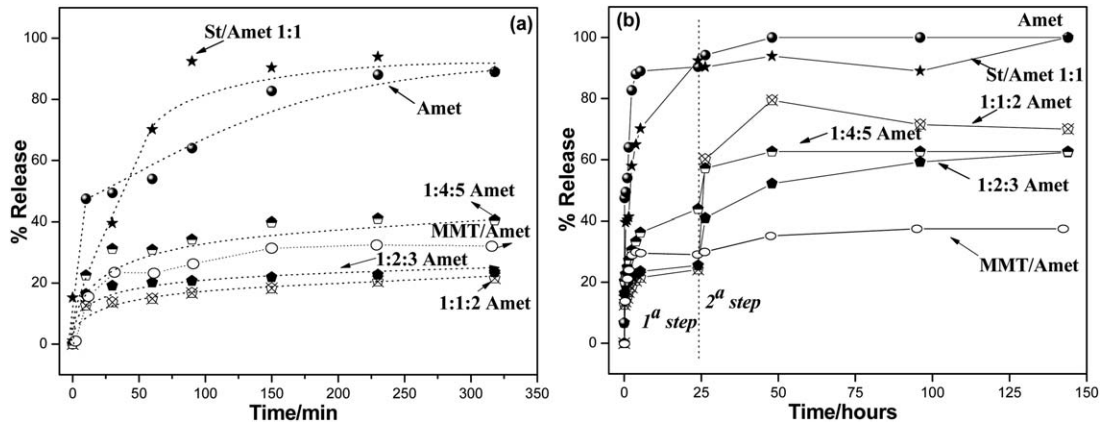

Figure 6. Release rate of ametryne as a function of time for pure ametryne and each of the composites at pH 7 and room temperature, first stage (**a**) and full curve (**b**).

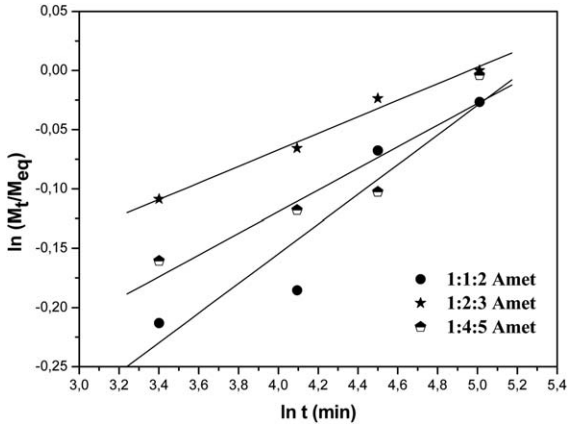

Figure 7. Results of the analyses of 1 : 1 : 2, 1 : 2 : 3, and 1 : 4 : 5 Amet nanocomposites containing ametryne, using the mathematical model of Peppas.

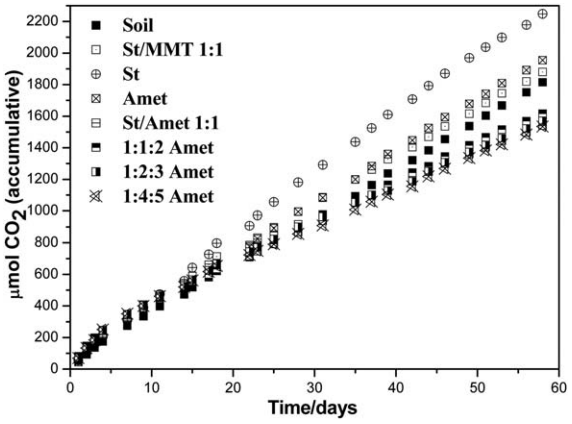

Figure 8. Evolution of CO_2 for starch gel (St), ametryne (Amet) and nanocomposites containing ametryne.

second releasing mechanism was shown. It may be related to the hydration of the starch chains, since this biopolymer is highly hydrophilic, leading to its dissolution. Then, in this case, the herbicide retained by the encapsulation would be free to solubilize in the aqueous medium, and the final retention observed would be related only to the MMT effect. In order to understand the release mechanisms, experiments to estimate the diffusion behavior were done, according to those proposed by Singh et al.[14] The release of a compound associated with nanoparticles involves several mechanisms, including desorption from the surface of the polymeric matrix, diffusion of active ingredients through the pores of the polymer matrix or the polymer wall, the disintegration of the nanoparticles and subsequent release of the active ingredients and dissolution and erosion of the polymer matrix or wall. Figure 7 shows the slope of ln (M_t/M_{eq}) × ln t at pH 7.0 for nanocomposites containing ametryne, which is useful to determine the diffusional exponent (n) and diffusion constant (k), according to the equation proposed by Serra et al.[32] [eq. (2)].

Rigter and Peppas[17] described mathematical models to analyze the release characteristics of substances in polymeric systems. Generally this equation is often employed in the absence of information on the delivery system mechanism. The adjusted values, as shown in Table IV, reveal that the releasing constant (k) does not change significantly with the MMT addition. It is noteworthy that the samples with ametryne showed a higher k value, which is expected, since in its dissolution the water diffusion into the structure will be facilitated. Small variations in the diffusional exponent (n) were observed for the St/MMT nanocomposites, which may indicate that the starch swelling is the mechanism governing the diffusion.

However, it is worth mentioning that in the St/MMT/Amet nanocomposites, n reduced in higher contents of MMT, indicating that the dispersed clay imposed a restriction for the diffusional water movement in the nanocomposite. This result is very important, since it shows that the MMT effect is mainly associated to the herbicide, and not to the starch. Finally, this is important to show the cooperative association of starch and MMT in those releasing systems (Table IV).

The influence of MMT incorporation on the biodegradation of starch gel and ametryne was investigated. Figure 8 shows the temporal CO_2 evolution in a compost soil. The degradation extension was quite similar among the samples in the initial period. The differences were observed after 20 days of composting: MMT addition retarded the starch and ametryne biodegradation since neat ametryne and neat starch present higher CO_2 evolution than St/MMT 1 : 1 or 1 : 1 : 2, 1 : 2 : 3, and 1 : 4 : 5 Amet nanocomposites. This event is due to possible van der Waals interactions between starch and ametryne and the clay and ametryne, such as observed in the FTIR results.

Table IV. Release Constants (k), Correlation Coefficient, and Diffusion Exponent Obtained by Adjusting the Curves of the Release Kinetics of the Herbicides Encapsulated in the Nanocomposites

Parameters	1 : 1 : 2 Amet	1 : 2 : 3 Amet	1 : 4 : 5 Amet
Release constant (k)	0.5191 s^{-1}	0.7070 s^{-1}	0.6161 s^{-1}
Diffusional exp. × 10^{-2}	12.52	6.99	0.91
Correlation coefficient	0.9432	0.9918	0.9372

CONCLUSIONS

In summary, nanocomposite based on MMT exfoliated into a starch matrix and incorporating a high amount of ametryne (50% in herbicide mass weight) was studied, in order to control the release of this herbicide. The good interactions between both components of biodegradable nanocomposite of starch/montmorillonite/ametryne show that it is possible to use starch (matrix) and montmorillonite (load) in a synergistic way, obtaining a processable system. By results obtained from the release rate of active components in water it was possible to observe both components in the nanocomposite playing a role in the herbicide release. The nanocomposite structural analysis gave evidence that the release behavior is governed by the

interaction between the constituents, even at very high herbicide contents. The nanocomposite biodegradation also confirms the potential of this material for practical applications.

ACKNOWLEDGMENTS

The authors are grateful to Embrapa-Brazil, Fapesp, CNPq, and Capes for grants, scholarship, and financial supports.

REFERENCES

1. Levine M. J. Pesticides: a toxic time bomb in our midst. In Library of Congress Cataloging-in-Publication Data; Praeger: USA, **2007**, p 1.
2. Arias-Estévez, M.; López-Periago, E.; Martínez-Carballo, E.; Simal-Gándara, J.; Mejuto, J.; García-Río, L. *Agric. Ecosyst. Environ.* **2008**, *123*, 247.
3. Canle, M. L.; Rodríguez, S.; Vázquez, L. F. R.; Santaballa, J. A.; Steenken, S. *J. Mol. Struct.* **2001**, *565*, 133.
4. Fernández-Pérez, M.; Flores-Céspedes, F.; González-Pradas, E.; Villafranca-Sánchez, M.; Pérez-García, S.; Garrido-Herrera, F. J. *J. Agric. Food Chem.* **2004**, *52*, 3888.
5. Mills, M. S.; Thurman, E. M. *Environ. Sci. Technol.* **1994**, *28*, 600.
6. Sopenã, F.; Cabrera, A.; Maqueda, C.; Morillo, E. *J. Agric. Food Chem.* **2007**, *55*, 8200.
7. Wienhold, B. J.; Gish, T. *J. Chemosphere* **1994**, *28*, 1035.
8. Carr, M. E.; Wing, R. E.; Doane, W. M. *Cereal Chem.* **1992**, *68*, 262.
9. El Bahri, Z.; Taverdet, J. L. *Polym. Bull.* **2005**, *54*, 353.
10. Smith, D.T.; Richard Jr, E. P.; Santo, L. T. The Triazine Herbicides, 50 years Revolutionizing Agriculture. In Weed Control in Sugarcane and the Role of Triazine Herbicides; LeBaron, H. M., McFarland, J. E., Burnside, O. C., Eds.; Elsevier: New York, **2008**, p 185.
11. Pereira, E. I.; Minussi, F. B.; Cruz, C. C. T.; Bernardi, A. C. C.; Ribeiro, C. *J. Agric. Food Chem.* **2012**, *60*, 5267.
12. Lu, P. F.; Zhang, M.; Liu, Y.; Li, J. L.; Xin, M. *J. Appl. Polym. Sci.* **2012**, *126*, 116.
13. Gerstln, Z.; Nasser, A.; Mingelgrin, U. *J. Agric. Food Chem.* **1998**, *46*, 3803.
14. Singh, B.; Sharma, D. K.; Kumar, R.; Gupta, A. *Appl. Clay Sci.* **2009**, *45*, 76.
15. American Society for Testing and Materials (ASTM). ASTM D570-98. In: 2002 Annual book of ASTM standards; ASTM: West Conshohocken (PA), **2002**.
16. Aouada, F. A.; Muniz, E. C.; Vaz, C. M. P.; Mattoso, L. H. C. *Quim. Nova* **2009**, *32*, 1482.
17. Ritger, P. L.; Peppas, N. A. *J. Control. Release* **1987**, *5*, 23.
18. Tomaszewska, M.; Jarosiewicz, A. *J. Agric. Food Chem.* **2002**, *50*, 4634.
19. Associação Brasileira de Normas Técnicas, Resíduos em solo—Determinação da biodegradação pelo método respirométrico, ABNT-NBR-14283, **1999**.
20. Campos, A.; Martins-Franchetti, S. M.; Marconato, J. C.; Agnelli, J. A. M.; Monteiro, M. R. *Res. J. Biotech.* **2007**, *2*, 20.
21. Cerqueira, V. S.; Hollenbach, E. B.; Maboni, F.; Vainstein, M. H.; Camargo, F. A. O.; Peralba, M. D. C. R.; Bento, F. M. *Bioresour. Technol.* **2011**, *102*, 11003.
22. Campos, A.; Teodoro, K. B. R.; Teixeira, E. M.; Corrêa, A. C.; Marconcini, J. M.; Wood, D. F.; Williams, T. G.; Mattoso, L. H. C. *Polym. Eng. Sci.* **2013**, *53*, 800.
23. Besün, N.; Peker, S.; Köktürk, U.; Yilmaz, H. *Colloid Polym. Sci.* **1997**, *275*, 378.
24. Ibrahim, S. M. *J. Appl. Polym. Sci.* **2011**, *119*, 685.
25. Chapple, S.; Anandjiwala, R.; Sinha Ray, S. *J. Thermal Calorim.* **2013**, *113*, 703.
26. Schlemmer, D.; Angélica, R. S.; Sales, M. J. A. *Compos. Struct.* **2010**, *92*, 2066.
27. Aouada, F. A.; Mattoso, L. H. C.; Longo, E. *Ind. Crop. Prod.* **2011**, *34*, 1502.
28. Grillo, R.; Pereira, A. E.; de Melo, N. F.; Porto, R. M.; Feitosa, L. O.; Tonello, P. S.; Dias Filho, N. L.; Rosa, A. H.; Lima, R.; Fraceto, L. F. *J. Hazard. Mater.* **2011**, *186*, 1645.
29. Mano, J. F.; Koniarova, D.; Reis, R. L. *J. Mater. Sci.: Mater. Med.* **2003**, *14*, 127.
30. Senesi, N.; Testini, C. *Geoderma* **1982**, *28*, 129.
31. Wing, R. E.; Carr, M. E.; Doane, W. M.; Schreiber, M. M. In Polymeric Delivery Systems; EI-Nokaly, M. A., Piatt, D. M., Charpentier, B.A., Eds.; ACS: Washington DC, **1993**; Chapter 14, p 214.
32. Serra, L.; Doménech, J.; Peppas, N. A. *Biomaterial* **2006**, *27*, 5440.